Pergamon

Computers and Chemical Engineering Supplement (1999) S191–S194

PII: S0098-1354/99/00171-4

Stability and Transient Behavior of Homogeneous Azeotropic Distillation

Cornelius Dorn, Moonyong Lee†, Manfred Morari*
Automatic Control Laboratory, Swiss Federal Institute of Technology
ETH-Zentrum, CH–8092 Zürich, Switzerland

Abstract
In this article, the steady state and dynamic behavior of an azeotropic distillation column separating the homogeneous ternary mixture acetone-benzene-heptane is studied. Nonlinear phenomena reported in earlier studies like multiple steady states (Bekiaris et al., 1993) and limit cycles (Lee et al., 1999) are shown for this mixture. In addition, a new phenomenon is reported: the occurrence of homoclinic bifurcations resulting in cases of only one attractor in the presence of three steady states.
It is discussed how these phenomena are influenced by operating parameters such as distillate and reflux flow rate, feed composition, etc.. The steady state and dynamic behavior is classified in the parameter space.

Keywords: Azeotropic distillation, Multiple steady states, Instability, Oscillation, Hopf bifurcation, Homoclinic bifurcation.

INTRODUCTION

Azeotropic distillation is an important separation technique which finds wide use in industry. The steady state and dynamic behavior of azeotropic distillation have been studied extensively over the past decades. This understanding is a necessary prerequisite for proper column design and operation. It has been shown that azeotropic distillation columns can exhibit unusual features not observed in non-azeotropic distillation (e.g. Laroche et al. (1992)). In particular, multiplicity of steady states has been the focus of much recent research. The existence of multiple solutions in azeotropic distillation is now widely accepted both by theoreticians and practitioners. Throughout this work, the term "multiple steady states" (MSS) refers to output multiplicities only.
A short overview of research related to the oscillatory behavior in azeotropic distillation is given in Lee et al. (1999). Recently, Lee et al. (1999) published simulation results showing sustained oscillations (limit cycles) in the homogeneous azeotropic distillation of methanol-methyl butyrate-toluene using a CMO model. The results obtained with the CMO model were reconfirmed with a more complex model (RADFRAC in AspenDynamics) and two different VLE models.
The main emphasis in this paper is to understand how system parameters influence the multiplicity and oscillatory behavior of a homogeneous azeotropic distillation column. It will be shown that the column can have an even more complex bifurcation behavior than shown in the earlier study by Lee et al. (1999).

SIMULATION SETUP

Mixture and Column Model

The ternary homogeneous mixture acetone-benzene-heptane investigated by Bekiaris et al. (1993) is chosen for the simulation study. The mixture belongs to the class 001 according to Matsuyama and Nishimura (1977). Acetone and heptane form the only minimum boiling binary azeotrope in this mixture at 93.56% (molar) acetone. The constant molar overflow (CMO) model is chosen (for details see e.g. Lee et al. (1999)). Data for the simulation are given in Table 1. Vapor pressures and liquid activity coefficients are calculated with the Antoine equation and Wilson model, respectively. The thermodynamic parameters are taken from Güttinger and Morari (1996). For the dynamic simulations the CMO model is integrated with DDASAC (Stewart et al., 1995), an index-1 DAE solver. For the steady state bifurcation analysis, the CMO model is incorporated into AUTO (Doedel *et al.*, 1997). To investigate the local dynamic behavior and stability, the nonlinear CMO model is linearized and the eigenvalues are calculated with LAPACK (Anderson et al., 1995) at every steady state. The average tray temperature T_{avg} is chosen as a scalar index for the bifurcation diagrams and dynamic simulations.

Number of trays (including condenser and reboiler)	46
Feed tray (counting from condenser)	41
Tray liquid hold-up [kmol]	3
Condenser liquid hold-up [kmol]	3
Reboiler liquid hold-up [kmol]	3
Column pressure [atm]	1.0
Feed flow rate [kmol/h]	100

Table 1: Column data for simulation

Parameterization of the Column Model

The number of parameters needed to specify an actual distillation column model makes a complete parametric study impractical. However, once a mixture is given, it is possible to demonstrate the more relevant parametric effects by using appropriate dimensionless variables. The set of nonlinear coupled ODEs which describe the chosen CMO model for a ternary mixture can be rewritten in a compact vector form: $d\mathbf{x}/dt' = \mathbf{f}(\mathbf{x}, D', \mathbf{P})$, where $t' = t/(M/F)$ is the dimensionless time. Further, $\mathbf{x} = (x_L^1, x_H^1, x_L^2, x_H^2, \cdots, x_L^N, x_H^N)^T$ is the composition vector of the liquid phases, $D' = D/F$ is the dimensionless distillate rate used as the bifurcation

†School of Chem. Eng. and Tech., Yeungnam University, Dae-Dong 214-1, Korea.
*Author to whom correspondence should be addressed. Phone: +41 1 632–2271. Fax: +41 1 632–1211.
Email: morari@aut.ee.ethz.ch

variable, and $\mathbf{P} = (L', x_I^F, x_{LH}^F)^T$ is the vector of operating parameters with $L' = L/F$ as the dimensionless reflux rate, x_I^F as the entrainer fraction in the feed, and $x_{LH}^F = x_L^F/x_H^F$ as the ratio of light and heavy component fraction in the feed.

INFLUENCE OF OPERATING PARAMETERS ON BIFURCATION BEHAVIOR

In order to understand how changes in the operating parameters L', x_I^F, and x_{LH}^F influence the multiplicity and oscillatory behavior, a parametric study is carried out.

MSS Region

With the ∞/∞ analysis (Bekiaris et al., 1993) it can be predicted that for the feed mixture studied here there will be multiple steady states for all feed compositions as long as the column is sufficiently long and the reflux is sufficiently high. Further, the location of the left and right turning points D'_{L1} and D'_{L2} can be predicted for the ∞/∞ case (infinite number of trays, infinite reflux flow rate) to be at:

$$D'_{L1} = \frac{x_{LH}^F}{1 + x_{LH}^F} \cdot (1 - x_I^F) \tag{1}$$

$$D'_{L2} = \begin{cases} \frac{x_{LH}^F}{1+x_{LH}^F} \cdot \frac{1-x_I^F}{x_L^{az}} & x_{LH}^F \le x_{LH}^{az} \\ (1 - x_I^F) & x_{LH}^F \ge x_{LH}^{az} \end{cases} \tag{2}$$

In the above equation, x_{LH}^{az} denotes the ratio of light to heavy component in the binary acetone-heptane azeotrope (≈ 14.5).

Effect of Light/Heavy Fraction. In the ∞/∞ case, both turning points are moved towards larger values of D' and the size of the MSS region increases as x_{LH}^F is increased until $x_{LH}^F = x_{LH}^{az}$. As x_{LH}^F is increased further, the right turning point D'_{L2} remains while D'_{L1} is still increasing. Hence the MSS region becomes narrower. Figure 1 shows bifurcation diagrams varying x_{LH}^F for several values of x_I^F. The behavior of the MSS regions is in good qualitative agreement with the predictions.

Effect of Entrainer Fraction. In the ∞/∞ case, both turning points are moved towards larger values of D' and the size of the MSS region increases as x_I^F is decreased. The results of a bifurcation analysis varying x_I^F for several values of L' are shown in Figure 2. As it can be seen, the MSS region moves toward higher D' as x_I^F decreases for given L'. However, the MSS region initially expands and then narrows as x_I^F decreases whereas the ∞/∞ analysis predicts a monotonic expansion. This discrepancy is due to the finite reflux flow rate and finite number of trays in the simulations.

Effect of Reflux Rate. For the example studied here multiplicities occur for all possible feed compositions if L' is sufficiently large and the column has enough trays. As L' decreases, the MSS region becomes smaller and finally disappears due to insufficient separation.

Dynamic Behavior

In this section, the steady states will be classified according to the eigenvalues of the local linearizations. The eigenvalue(s) with the largest real part will be referred to as *dominant*. In all cases studied where the dominant eigenvalue was real, the real part of the closest complex eigenvalue was significantly smaller. Thus, it is sufficient to study the dominant eigenvalue for a classification of the dynamic behavior. Regions on the steady-state branches where the dominant eigenvalue is complex (i.e. either damped or sustained oscillation) are bounded by stars in the bifurcation plots.

Effect of Light/Heavy Fraction. The bifurcations plotted in Figure 1 show that the influence of x_{LH}^F is mainly to shift the MSS region towards higher values of D'. The characteristic features (e.g. region of oscillation or occurrence of Hopf bifurcation points) are nearly unaffected.

Effect of Entrainer Fraction. As illustrated in Figure 2, the dominant eigenvalue for steady states on the low branch was always negative real (stable node). For steady states on the middle branch, it was always positive real (unstable).

For large values of x_I^F, the steady states on the high branch are all stable nodes. As x_I^F is decreased, a region appears and becomes more apparent on the high branch where the steady states have a complex dominant eigenvalue. Time responses starting close to those steady states will show underdamped oscillations. As x_I^F is further decreased, two Hopf bifurcation points appear in the region of oscillation. The steady states on the high branch in the region between the two Hopf bifurcation points are unstable and surrounded by stable limit cycles.

Next, two homoclinic bifurcation points appear on the high branch between the two Hopf bifurcation points. Therefor the interval of D' where stable limit cycles exist is disconnected by a region where the limit cycles disappear, as illustrated in Figure 4 (This interval is not illustrated in Figures 1 and 2 for clarity). For values of D' in this interval this results in one stable and two unstable steady states, the former being the only attractor. In Figure 4, the vertical distance between the dots depicts the amplitude of the limit cycles. The coalescence of limit cycles with the middle branch essentially causes the limit cycles to disappear. Figure 5 illustrates the time response of T_{avg} to consecutive step changes.

As shown in Figure 2, the region limited by the Hopf bifurcation points expands further until for some value of x_I^F the left Hopf bifurcation point and the left homoclinic bifurcation point together reach the left turning point and disappear. Then, a region where the dominant eigenvalue is positive real will appear on the high branch between the left turning point and the homoclinic point (Figure 2c) thus disconnecting the region of oscillation. The resulting left region of oscillation shrinks towards the left turning point and disappears while the right oscillation region becomes gradually narrower (Figure 2d).

Effect of Reflux Rate. As illustrated in Figure 2, the main characteristic features of the bifurcation also changes significantly with increasing L'. When x_I^F is smaller than some critical value, the qualitative effect of increasing L' is the same as that of decreasing x_I^F: first a region of oscillation appears on the high branch and gets larger, then a region of unstable steady states surrounded by stable limit cycles appears within the region of oscillation, and so on.

Effect of Other Parameters. The size of both the

MSS region and the region of oscillation is increased as the number of trays in the column increases. The liquid hold-up directly affects the period of oscillation.

CLASSES OF DYNAMIC BEHAVIOR

In the preceding section, it was shown that the qualitative bifurcation behavior is mainly influenced by L' and x_I^F whereas the main effect of x_{LH}^F is to simply shift both the MSS region and the region of oscillations without changing their main characteristics. This allows to focus on L' and x_I^F to characterize the types of dynamic behavior. In this section, it will be studied how the (L', x_I^F) parameter space is divided into regions corresponding to qualitatively different steady state and dynamic behavior. For the example studied in this paper, the regions are illustrated in Figure 3.

Region I. For values of (L', x_I^F) in region I, there is a unique steady state for every D'. All steady states are stable.

Region II. In subregion II-a, MSS exist but no oscillations occur throughout the high branch. All the dominant eigenvalues are real. In subregion II-b, damped oscillation appears for some range of D' on the high branch.

Region III. This region also consists of two subregions. Subregion III-a is a narrow band at the border with region II (not illustrated separately). For values of L' and x_I^F in this region, there are two Hopf bifurcation points on the high branch. All steady states between these two Hopf bifurcation points are unstable and surrounded by stable limit cycles.

Subregion III-b consists of the remainder of region III and exhibits an interesting phenomenon newly observed in distillation: the occurrence of homoclinic bifurcation points. The amplitude of the limit cycles around the high branch grows until the limit cycles touch the middle branch. The interval of D' between the Hopf bifurcation points is therefore disconnected by an interval bounded by the two homoclinic bifurcation points where the limit cycles disappear, as illustrated in Figure 4. This results in one stable and two unstable steady states, the former being the only attractor.

As L' is further increased (or x_I^F further decreased) in region III, the left Hopf bifurcation point and the left homoclinic bifurcation point approach the left turning point.

Region IV. For values of (L', x_I^F) in region IV, there is only one Hopf bifurcation point on the high branch. The steady states to the right of the Hopf bifurcation point are stable. The interval of the high branch between the left turning point and the Hopf bifurcation point consists of two parts separated by a homoclinic bifurcation point: The unstable steady states in the right part are surrounded by stable limit cycles whereas there are no limit cycles around the unstable steady states in the left part.

The simulations revealed that oscillations are most likely to occur on the high branch under the condition of small x_I^F and large L'. The occurrence of oscillation seems to be closely related to the distribution of entrainer inventory inside the column. Small x_I^F and large L' result in an entrainer profile with a sharp large peak. In this part of the column there is steep front in the temperature profile bounded by well developed pinch zones.

CONCLUSIONS

In this paper, it was shown that homogeneous azeotropic distillation can exhibit complex steady state and dynamic behavior. Based on the CMO model, it was studied how process operation affects the characteristic features of multiplicity and stability. It was observed that both x_I^F and L' have a significant effect on the qualitative bifurcation behavior. In comparison, the effect of x_{LH}^F is to shift the MSS and oscillation regions. The (L', x_I^F) parameter space is divided into four regions according to the main features of bifurcation behavior. A new phenomenon in homogeneous distillation was discovered: the occurrence of homoclinic bifurcation points. Thus, for certain sets of operating parameters there exist three steady states with only one attractor.

NOTATION

F	Molar feed flow rate
$D' = \frac{D}{F}$	Dimensionless distillate flow rate
$L' = \frac{L}{F}$	Dimensionless reflux flow rate
x_c^n	Molar liq. frac. of component c on tray n
T_{avg}	Average temperature of all trays
$t' = t\frac{F}{M}$	Dimensionless time
M	Molar liquid holdup on a tray
N	Number of trays
x^F	Molar feed composition
x_{LH}^F	Ratio of the feed light to heavy comp. frac.
x_c^{az}	Molar liq. frac. of comp. c of azeotrope
x_{LH}^{az}	Ratio of the az. light to heavy comp. frac.

Acknowledgement

This work was supported by the KOSEF through the Automation Research Center at POSTECH and by the KOSEF - Swiss National Science Foundation exchange program.

REFERENCES

Anderson, E.; Bai, Z.; Bischof, C.; Demmel, J.; Dongarra, J. Lapack Users' Guide: Release 2.0, International Society for Industrial and Applied Mathematics.

Bekiaris, N.; Meski, G. A.; Radu, C. M.; Morari, M. *Ind. Eng. Chem. Res.* **1993**, *32*(9), 2023.

Doedel, E.J.; Champneys, A.R.; Fairgrieve, T.F.; Kuznetsov, Y.A.; Standstede, B. and X. Wang (**1997**). AUTO97: *Continuation and Bifurcation Software for Ordinary Differential Equations.* Concordia University. Montreal, Canada. Software documentation.

Güttinger, T. E.; Morari, M. *Ind. Eng. Chem. Res.* **1996**, *35*(3), 2816.

Laroche, L.; Bekiaris, N.; Andersen, H. W.; Morari, M. *AIChE Journal* **1992**, *38*(9), 1309.

Lee, M.; Dorn, C.; Meski, G. A.; Morari, M. Limit Cycles in Homogeneous Azeotropic Distillation, *Accepted for Ind. Eng. Chem. Res.* **1999**.

Matsuyama, H.; Nishimura, H. *J. Chem. Eng. Jpn.* **1977**, *10*(3), 181.

Stewart, W. E.; Caracotsios, M.; Sorensen, J. P. DDASAC Software Package Documentation, University of Wisconsin, Madison, WI 53706, USA, **1995**.

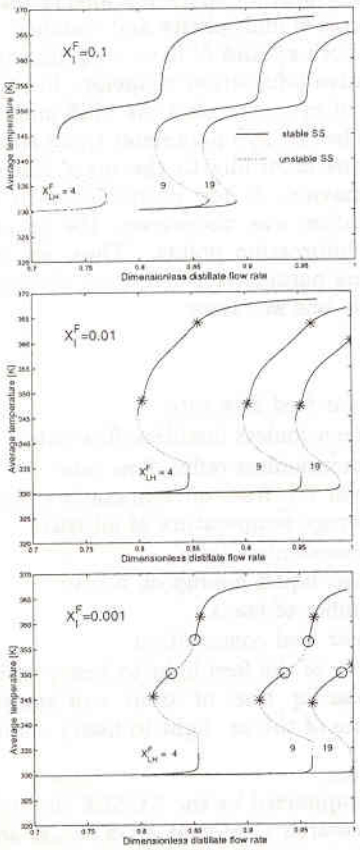

Figure 1: Influence of x_{LH}^F on the multiplicity and oscillatory behaviors: L'=12; the oscillations occur in the region bounded by the two *s; o denotes Hopf bifurcation points.

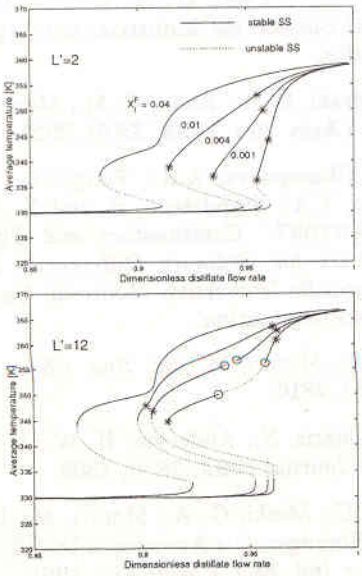

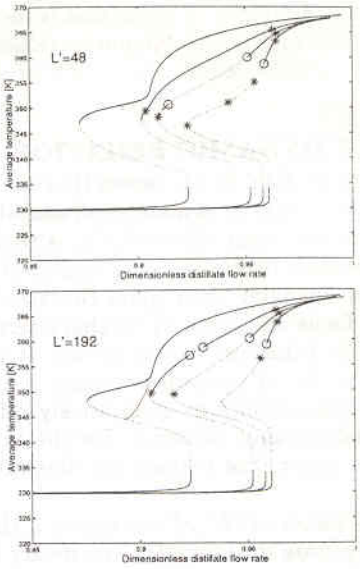

Figure 2: Influence of L' and x_I^F on the multiplicity and oscillatory behaviors: x_{LH}^F=9; the oscillations occur in the region bounded by the two *s; o denotes Hopf bifurcation points.

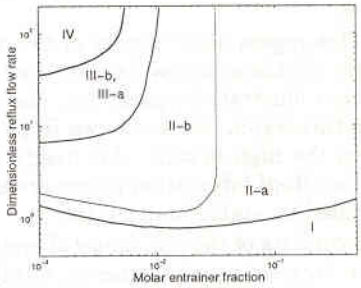

Figure 3: Classification of dynamic behavior in parameter space $L' - x_I^F$: x_{LH}^F=9.

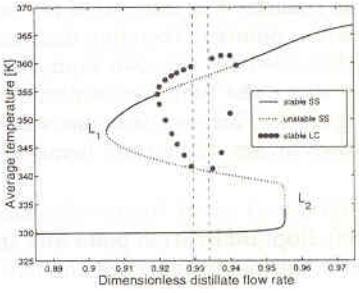

Figure 4: Steady state bifurcation diagram (T_{avg} vs D') for region III : L'=48; x_I^F=0.007; x_{LH}^F=9.

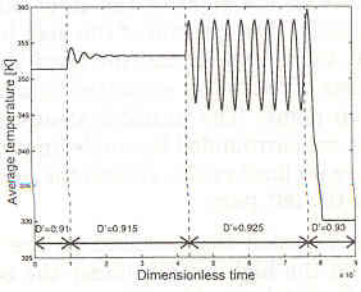

Figure 5: Response of average temperature in the column to consecutive step changes in D': L'=48, x_I^F=0.007, x_{LH}^F=9. ($t' = 33.3 \hat{=} t = 1$h).